GLOBAL LAND SURFACE EVAPORATION FROM SATELLITE-BASED OBSERVATIONS

Diego G. Miralles, Richard de Jeu, Thomas Holmes[*]*, John Gash, Han Dolman*[†]

Vrije Universiteit Amsterdam
Department of Hydrology and GeoEnvironmental Sciences
De Boelelaan 1085, 1081 HV, Amsterdam, NL

1. INTRODUCTION

Estimating the magnitude of the different fluxes in the hydrological cycle is essential if we are to predict the impacts of climate change. However, climate change is acting on a dynamic three dimensional globe where change in one region may produce impacts in another. This creates a need to expand the current climate change studies to encompass the entire globe. Evaporation is a key component of the hydrological cycle as it can affect both feedbacks on large scale water processes (e.g.[1]) and the dynamics of the atmosphere due to changes in the Bowen ratio (e.g.[2]).

The uncertainty in predictions of future climate must be reduced if we want to effectively manage adaptation to climate change. Consequently, there is a need to create observation-based benchmarks, against which GCM performance can be judged (e.g.[3]). Hydro-meteorological benchmarks will allow selection between GCMs and lead to improvement in model simulations of the hydrological cycle. The first priority is to combine the available remote sensing data products with hydrological models and land surface parameterization schemes to create such an evaporation benchmark.

In the last two decades several attempts have been made to build global evaporation products using remote sensing information. In 1997, Choudhury pioneered a potential evaporation product based on data assimilation of satellite observations ([4]). His approach applied the Penman-Monteith equation and derived monthly evaporation maps for the years 1987 and 1988. Years later [5] also used the Penman-Monteith equation to derive global evaporation, but applying more advanced remote sensing products from the MODIS sensor.

Several model and satellite-based evaporation products are now available, but the majority of these models lack the key elements of estimating forest rainfall interception loss and the coupling of transpiration with observed soil moisture. Global Land surface Evaporation: the Amsterdam Model (GLEAM), a unique methodology to derive evaporation from remotely sensed observations, has been developed at the VU University of Amsterdam to fill these gaps. GLEAM uses an extensive range of satellite observations as a basis for estimating daily actual evaporation at a global scale and 0.25 degree spatial resolution. Central to the approach is the Priestley and Taylor evaporation formula ([6]). This radiation-based model appears appropriate for the level of available driving data at the spatial scale of the study. The use of a variety of independent remote sense observations is only one of the main advantages of GLEAM over other evaporation models. Coupling of transpiration to soil moisture conditions and detailed, separate rainfall interception loss estimation are two key features that allow the approach to be applied in land-atmosphere feedback studies and tests of GCM performance. The proposed work describes the modeling framework and tests the applicability of the methodology in combination with the available remote sensing driving data. The final global evaporation flux has been validated, applying a selection of stations from the Fluxnet global network of micrometeorological flux measurements. Results corresponding to a wide range of years will be presented, showing the global spatial distribution of the model-estimated actual evaporation and analyzing the factors controling this distribution.

2. METHODOLOGY

Figure (a) illustrates the structure of GLEAM in four interconnected modules: 1) Interception model, 2) Soil water module, 3) Stress module, and 4) Priestley and Taylor module. The methodology is independently formulated for three main land surface types with specific physical processes: 1) land covered by tall canopies, 2) land covered by herbaceous vegetation, and 3) bare

[*] Thomas Holmes is currently working at USDA Agricultural Research Service, Hydrology and Remote Sensing Laboratory.

[†] This study is supported by the European Union (WATCH Integrated Project, 036946), and contributes to the Global Water System Project.

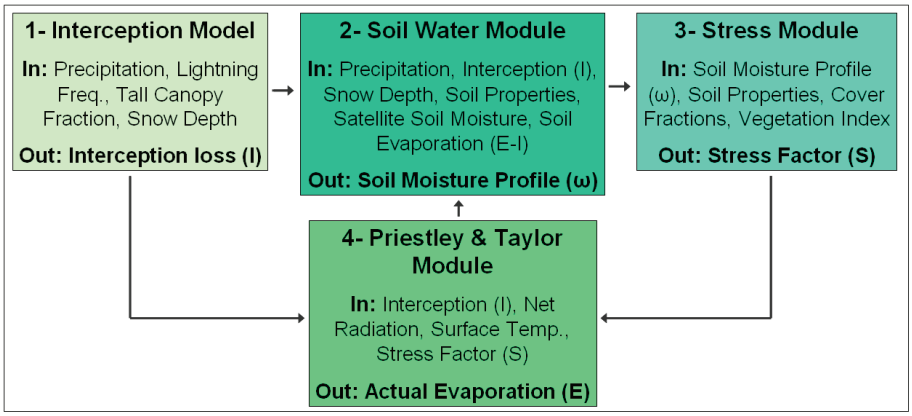

(a) Schematic overview of GLEAM

soil. The total evaporation is the aggregate of the evaporation values based on the cover fractions ([7]) of each land surface type within the pixel. Surfaces covered by ice or snow follow a separate routine in which sublimation is calculated.

2.1. Interception Model

The forest interception model is a completely independent part of GLEAM (it does not rely on the other three modules to produce estimates). GLEAM's interception model calculates daily global rainfall interception loss (I) based on ancillary data and is described in detail by [8]. The approach is based on the revised version of Gash's analytical model ([9]), driven by remotely sensed precipitation data (i.e. CMORPH dataset ([10])) and tall canopy fraction ([7]).

Under the assumption that lightning only occurs during convective storms, the Combined Global Lightning Flash Rate Density dataset from NASA is used to distinguish between synoptic and convective rainfall events and, therefore, to determine the value of the average rainfall rate and hence rainfall duration. This dataset merges the retrievals from the Optical Transient Detector (OTD) and the Lightning Imaging Sensor (LIS) ([11]) into a combined product consisting of a standard monthly climatology of lightning frequency (in number of flashes per square kilometer per year). Considering a linear relation between lightning frequency and fraction of rainfall of convective nature, the average rainfall rate is estimated at each particular pixel for every month of the year applying representative values of rainfall rate for convective and synoptic rainfall ([12]). The modelled I has been validated over 42 in situ observation sites, resulting in an overall correlation coefficient (R) of 0.86 and a negligible bias ([8]).

2.2. Soil Water Module

The soil water module is based on the implementation of a multilayer bucket model to estimate the soil moisture profile along the root zone. The first layer (which is set to 5cm depth) is assimilated with daily surface satellite soil moisture from AMSR-E ([13]) making use of an ensemble Kalman Filter. The infiltration flux into the running water balance is estimated using remote sensing precipitation data (i.e. CMORPH ([10])), snow depth (from the National Space and Ice Data Center (NSIDC)), internal rainfall interception (from the interception model) and internal soil evaporation (from the Priestley and Taylor module).

2.3. Stress Module

The function of the stress module is to translate the soil moisture profile into soil water stress conditions. The soil water stress is calculated as stress factor (S) ranging from 0 (maximum stress) to 1 (no stress). In the bare soil fraction the soil moisture in the top layer determines the water stress condition, while for vegetated cover fractions more weight is put on the wettest layer under the assumption that roots take water from where it is more easily available. Vegetation information (i.e. vegetation optical depth from microwave observations) is used to account for the effect of vegetation phenology in S.

2.4. Priestley and Taylor Module

Central part of GLEAM is the application of a Priestley and Taylor equation ([6]) to compute potential evaporation (E_p). This modelling of E_p is driven by remotely sensed products of net radiation (Surface Radiation Budget NASA/GEWEX) and land

surface temperature from passive microwave observations ([14]). The soil heat flux is defined as a fraction of net radiation. Modelled values of (E_p) are corrected using the estimates of (S) (from the stress module) and I (from the interception model) to produce actual evaporation (E): $E = E_p S + (1 - \beta)I$; where β is the interception coefficient and can be considered as a constant (β=0.07, see [15]).

3. RESULTS

3.1. Validation

The modelled (GLEAM) evaporation is compared to Fluxnet eddy covariance measurements at stations around the world ([15]). These stations cover the most common vegetation types and climates. A quality check on Fluxnet observations was applied resulting in a set of 40 reliable sites over a large variety of land uses. The validation over all the 40 sites, result in a median correlation coefficient of 0.85 and a 5% negative bias. For the comparisons with in situ Fluxnet stations only estimates of soil evaporation (I excluded) are considered, to cope with the fact that the reliability of eddy covariance observations is diminished during rain events (not allowing the correct measurement of the interception loss flux by the station). The independent validation of the GLEAM I estimates can be found in [8].

3.2. Global Application

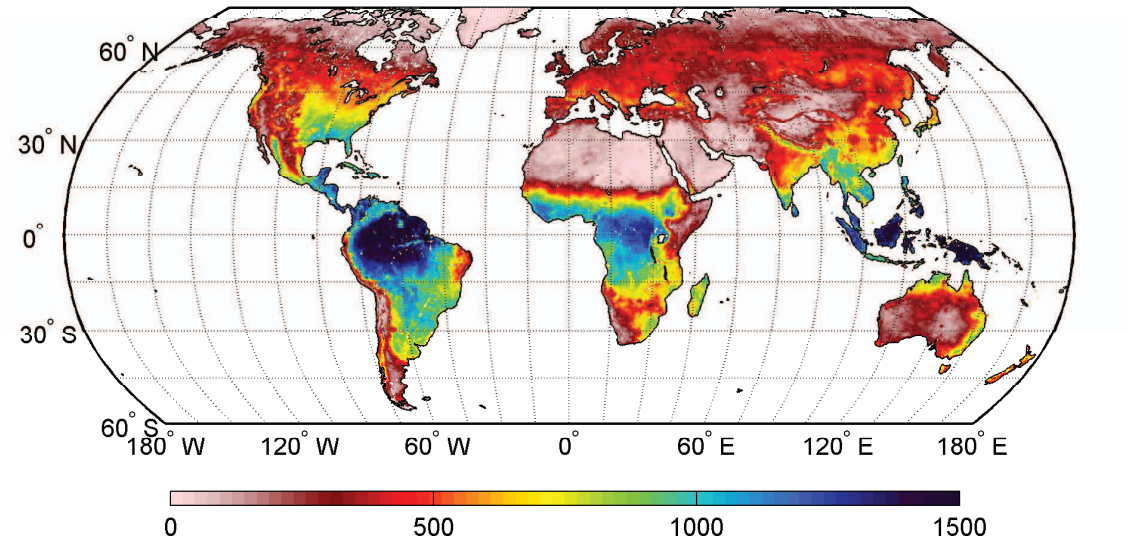

(b) Total GLEAM Evaporation (mm/year) for 2005

Figure (b) shows the cumulative global GLEAM evaporation (E, mm/year) for 2005 at 0.25 degree resolution. High values of evaporation (up to 1500 mm/year) can be found in the tropics and low values in the desert regions. At a continental scale E varies from about 59% of the total precipitation in South America to 71% in North America.

The contribution of rainfall interception loss to the total evaporation is significant. The largely forested areas within climatic zones in which rainfall is dominated by long-duration synoptic events (like Scandinavia or northern Canada), generally present the highest percentages of I (up to 30% of the total precipitation at annual basis). On the other hand, tropical forest areas, dominated by short duration convective rainfall events and large volumes of annual precipitation, present slightly lower percentages (with maximum values around 15%) ([16]).

4. CONCLUSION

A remotely sensed based methodology to estimate daily evaporation is presented. The approach uses the Priestley and Taylor evaporation equation in combination with an independent Gash-based rainfall interception model, and soil water and stress modules to create a dynamic global evaporation product. The results show high correlation with Fluxnet in situ observations

(median R=0.85) and low deviation (-5% average bias). The dataset is now ready for a few test years and before the end of the year 2010 it will span a period from 1983 to present.

5. REFERENCES

[1] G. Poveda and O. J. Mesa, "Feedbacks between hydrological processes in tropical South America and large-scale ocean-atmospheric phenomena," *Journal of Climate*, 1997, vol. 10, pp. 2690–2702.

[2] C. L. Dow and D. R. De Walle, "Trends in evaporation and Bowen ratio on urbanizing watersheds in eastern United States," *Water Resources Research*, 2000, vol. 36, pp. 1835–1843.

[3] E. M. Blyth, W. J. Shuttleworth, and R. J. Harding, "Summary of the GEWEX international symposium on global land-surface evaporation and climate," *Hydrological Processes*, 2009, vol. 23, pp. 3411–3412.

[4] B. J. Choudhury, "Global pattern of potential evaporation calculated from the Penman-Monteith equation using satellite and assimilated data," *Remote Sensing of Environment*, 1997, vol. 61, pp. 64–81.

[5] Q. Mu, F. A. Heinsch, M. Zhao, and S. W. Running, "Development of a global evapotranspiration algorithm based on MODIS and global meteorology data," *Remote Sensing of Environment*, 2007, vol. 111, pp. 519–1536.

[6] C. H. B. Priestley and R. J. Taylor, "On the assessment of surface heat flux and evaporation using large scale parameters," *Monthly Weather Review*, 1972, vol. 100, pp. 81–92.

[7] R. J. Joyce, J. E.Janowiak, P. A. Arkin, and P. Xiel, "CMORPH: A method that produces global precipitation estimates from passive microwave and infrared data at high spatial and temporal resolution," *Journal of Hydrometeorology*, 2004, vol. 5, pp. 487–503.

[8] D. G. Miralles, J. C. Gash, T. R. H. Holmes, R. A. M. De Jeu, and A. J. Dolman, "Global canopy interception from satellite observations," *Journal of Geophysical Research-Atmospheres*, accepted.

[9] F. Valente, J. S. David, and J. H. C. Gash, "Modelling interception loss for two sparse eucalypt and pine forests in central Portugal using reformulated Rutter and Gash analytical models," *Journal of Hydrology*, 1997, vol. 190, pp. 141–162.

[10] G. J. Huffman, R. F. Adler, M. M. Morrissey, D. T. Bolvin, S. Curtis, R. Joyce, B. McGavock, and J. Susskind, "Global precipitation at one-degree daily resolution from multisatellite observations," *Journal of Hydrometeorology*, 2001, vol. 2, pp. 36–50.

[11] D. M. Mach, H. J. Christian, R. J. Blakeslee, D. J. Boccippio, S. J. Goodman, and W. L. Boeck, "Performance assessment of the Optical Transient Detector and Lightning Imaging Sensor," *Journal of Geophysical Research-Atmospheres*, 2007, vol. 112.

[12] C. R. Lloyd, J. H. C. Gash, W. J. Shuttleworth, and F. A. de O. Marques, "The measurement and modelling of rainfall interception by Amazonian rainforest," *Agricultural and Forest Meteorology*, 1988, vol. 43, pp. 277–294.

[13] M. Owe, R. De Jeu, and T. Holmes, "Multisensor historical climatology of satellite-derived global land surface moisture," *Journal of Geophysical Research-Earth Surface*, 2008, vol. 113.

[14] T. R. H. Holmes, R. A. M. De Jeu, M. Owe, and A. J. Dolman, "Land surface temperature from Ka band (37 GHz) passive microwave observations," *Journal of Geophysical Research-Atmospheres*, 2009, vol. 114.

[15] J. H. C. Gash and J. B. Stewart, "Evaporation from Thetford Forest during 1975," *Journal of Hydrology*, 1977, vol. 35, pp. 385–396.

[16] D. Baldocchi, E. Falge, L. H. Gu, R. Olson, D. Hollinger, S. Running, P. Anthoni, C. Bernhofer, K. Davis, R. Evans, J. Fuentes, A. Goldstein, G. Katul, B. Law, X. H. Lee, Y. Malhi, T. Meyers, W. Munger, W. Oechel, K. T. P. U, K. Pilegaard, H. P. Schmid, R. Valentini, S. Verma, T. Vesala, K. Wilson, and S. Wofsy, "FLUXNET: A new tool to study the temporal and spatial variability of ecosystem-scale carbon dioxide and water vapor and and energy flux densities," *Bulletin of the American Meteorological Society*, 2001, vol. 82, pp. 2415–2434.